PHYSICAL REVIEW B **75**, 140511(R) (2007)

Switching the sign of Josephson current through Aharonov-Bohm interferometry

Fabrizio Dolcini and Francesco Giazotto
Scuola Normale Supèriore and NEST CNR-INFM, I-56126 Pisa, Italy
(Received 10 January 2007; published 24 April 2007)

The electromagnetostatic Aharonov-Bohm effect is proposed as a tool to realize a fully controllable Josephson π junction. Both the sign and the magnitude of the supercurrent can be tuned in a ring-shaped ballistic normal region coupled to superconducting electrodes by varying the magnetic flux and the electric field around suitable values. We provide a theoretical description of the system within the scattering matrix theory and discuss its implementation in a realistic setup.

DOI: 10.1103/PhysRevB.75.140511 PACS number(s): 74.50.+r, 73.23.−b, 85.25.Cp

The broad interest in mesoscopic physics has recently spurred a renewed impulse in the context of Josephson effect. Because of its large spectrum of applications to nanotechnology, the art of manipulating the supercurrent is presently under the spotlight. Josephson field-effect transistors, for instance, have been proposed[1] and realized both with semiconductors and carbon nanotubes.[2] A growing interest is nowadays devoted to the issue of supercurrent sign reversal: a π-junctions state, i.e., a Josephson current flowing in the direction opposite to the phase difference between the superconductors, has already been obtained with ferromagnet-superconductor (FS) junctions.[3] In these systems the sign of the current flow depends on the F-layer thickness, which cannot be varied during an experiment. In view of technological applications, the tunability of a system instead plays a crucial role, and the realization of *controllable* π junctions represents a major challenge both on the theoretical and experimental point of view. To this end, two approaches have been explored so far: tunable π states have been realized either by driving far from equilibrium the junction quasiparticle distribution function through current injection from additional terminals,[4] or by exploiting the electronic correlations in a quantum dot, where the electron number can be tuned through a gate.[5]

In this Rapid Communication, we present a different operational principle to implement a controllable π junction, which is based on the electromagnetostatic Aharonov-Bohm (AB) effect in a ballistic normal (N) ring coupled to two superconducting (S) leads. The proposed setup is shown in Fig. 1: the ring is treated by a magnetic flux Φ_B, and a gate voltage V_G is applied to one of the arms. Exploiting the magnetic or the electrostatic AB effect, one can tune the transmission of the ring and therefore manipulate the magnitude of the Josephson current. Here we show that if *both* the magnetic and the electric field are suitably applied, the *sign* of the supercurrent can be changed also. This leads to a fully controllable system operating at equilibrium, which exhibits potential for the implementation of low-dissipation transistors, quantum interference devices, as well as reduced-noise qubits.[6] Ideal candidates for the realization of the proposed setup are intermediate and/or long S-N-S junctions fabricated with $In_xGa_{1-x}As$ (with $x \geq 0.75$)[7] or InAs[8] rings, since they allow ballistic electron transport and lack of a Schottky barrier when contacted to metals, e.g., superconducting Nb.

We describe the system by setting the superconducting order parameter as $\Delta(x)=|\Delta|e^{-i\chi/2}$ in the left lead, $\Delta(x)=|\Delta|e^{+i\chi/2}$ in the right lead, and $\Delta(x)=0$ in the N region, where χ is the phase difference between the S electrodes. The Josephson current $J(\chi)$ of an S-N-S junction with an N region characterized by a Fermi velocity v_F^N and a length L can be written[9] as a sum of two contributions $J_d(\chi)$ and $J_c(\chi)$, arising from the discrete Andreev levels and the continuous spectrum, respectively. Explicitly, $J_{d,c}(\chi)=(2eE_L/\hbar)j_{d,c}(\chi)$, where $E_L=\hbar v_F^N/L$ is the energy associated with L (here the length of each ring arm), and

$$j_d(\chi) = \sum_p \tanh\left(\frac{\varepsilon_p \beta_L}{2}\right)\left(-\frac{\partial \varepsilon_p}{\partial \chi}\right), \tag{1}$$

$$j_c(\chi) = \frac{2}{\pi \beta_L}\int_{|\Delta_L|}^{\infty} d\varepsilon \ln\left[2\cosh\left(\frac{\varepsilon \beta_L}{2}\right)\right]\frac{\partial \,\mathrm{Im}[H(\varepsilon;\chi)]}{\partial \varepsilon}. \tag{2}$$

In Eqs. (1) and (2) energies are expressed in terms of E_L, so that $|\Delta_L|=|\Delta|/E_L$, $\varepsilon=(E-E_F)/E_L$ is the energy variation with respect to the Fermi level E_F of leads and N region, and $\beta_L=E_L/k_BT$ is the inverse temperature. The Andreev levels $\varepsilon_p(\chi) \in [0;|\Delta_L|]$ in Eq. (1) are determined by the solutions of $D(\varepsilon;\chi)=0$,[10] where the function

$$D(\varepsilon;\chi) = \det[\mathbb{1} - A(\varepsilon) r_A^*(\chi) \mathsf{S}(\varepsilon) r_A(\chi) \mathsf{S}^*(-\varepsilon)] \tag{3}$$

accounts both for the dynamics in the N region, through the particle (hole) scattering matrix $\mathsf{S}(\varepsilon)$ ($\mathsf{S}^*(-\varepsilon)$), and for the Andreev reflections at the S contacts through the matrix $r_A(\chi)=\mathrm{diag}(e^{i\chi/2}, e^{-i\chi/2})$ and the amplitude $A(\varepsilon)$, which

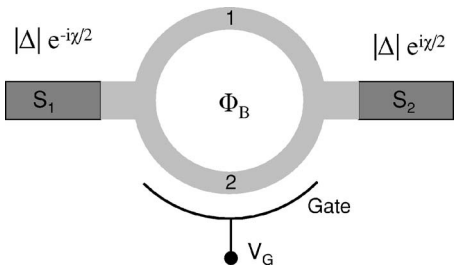

FIG. 1. Scheme of the Aharonov-Bohm Josephson junction. Light gray region indicates the normal metal ring, whereas dark gray denotes the superconducting leads.

equals $\exp(-2i\arccos(\varepsilon/|\Delta_L|))$ for $|\varepsilon|<|\Delta_L|$ and $(\varepsilon-\sqrt{\varepsilon^2-|\Delta_L|^2})/(\varepsilon+\sqrt{\varepsilon^2-|\Delta_L|^2})$ for $|\varepsilon|>|\Delta_L|$. Finally, the function H appearing in Eq. (2) reads

$$H(\varepsilon;\chi)=\partial_\chi \ln D(\varepsilon;\chi). \tag{4}$$

Although general, Eqs. (1) and (2) do not allow a straightforward evaluation of $J(\chi)$ for an arbitrary S matrix, for the determination of the Andreev levels may be a formidable task. In the limit of short junction $|\Delta_L|\ll 1$, however, Beenakker showed that the contribution (2) vanishes, and that the evaluation of the Andreev levels in Eq. (1) is considerably simplified. He thus proved[9] that in this limit and for a symmetric S matrix, the Josephson current acquires a simple expression in terms of the transmission coefficients $\mathcal{T}_i$'s of S. In a typical experimental realization of the setup of Fig. 1, however, the short junction regime $|\Delta_L|\ll 1$ is not achieved; as observed above, one rather has $|\Delta_L|\gtrsim 1$. Furthermore, in the presence of a magnetic flux, the ring S matrix is not symmetric in general. It is therefore important to analyze the behavior of the Josephson current also beyond the short-junction limit, and without assuming the symmetry of the S matrix. To this purpose, it is suitable to rewrite Eqs. (1) and (2) in a different way. Here we briefly sketch the main steps of our strategy, based on analytic continuation of Eq. (4) in the complex plane.[11] We first observe that, due to causality,[12] the scattering matrix $\mathsf{S}(\varepsilon)$ has an analytic continuation $\mathsf{S}(z)$ in the upper complex half plane $\mathrm{Im}(z)>0$. Then, elementary properties of holomorphic functions lead to prove that $H_{\mathrm{R}}(z;\chi)\doteq\partial_\chi \ln D_{\mathrm{R}}(z;\chi)$ and $H_{\mathrm{A}}(z;\chi)\doteq\partial_\chi \ln D_{\mathrm{A}}(z;\chi)$ with

$$D_{\mathrm{R}}(z;\chi)=\det[\mathbb{1}-A(z)r_A^*(\chi)\mathsf{S}(z)r_A(\chi)(\mathsf{S}(-z^*))^*], \tag{5}$$

$$D_{\mathrm{A}}(z;\chi)=\det[\mathbb{1}-A(z)r_A(\chi)(\mathsf{S}(z^*))^* r_A^*(\chi)\mathsf{S}(-z)] \tag{6}$$

are analytic continuations of Eq. (4) for $\mathrm{Im}(z)>0$ and $\mathrm{Im}(z)<0$, respectively. Here $A(z)$ is the continuation of $A(\varepsilon)$ with a branch cut in $z\in[-|\Delta_L|;|\Delta_L|]$. The relation $H_{\mathrm{R}}(\varepsilon+i0^+)=H_{\mathrm{A}}(\varepsilon+i0^-)$ for $|\varepsilon|<|\Delta_L|$ stemming from Eqs. (5) and (6), together with equality $\partial_\chi\varepsilon_p=-\partial_\chi D(\varepsilon_p;\chi)/\partial_\varepsilon D(\varepsilon_p;\chi)$ for the Andreev levels, allows one to rewrite Eq. (1) as

$$j_{\mathrm{d}}(\chi)=\frac{1}{2\pi i}\sum_{\eta=\mathrm{R,A}}\sum_p\int_{\Gamma_\eta^p}\tanh\left(\frac{z\beta_L}{2}\right)H_\eta(z,\chi)dz, \tag{7}$$

where Γ_R^p (Γ_A^p) is a small semicircular contour around ε_p, in the upper (lower) half plane. Similarly, the relation $H_{\mathrm{R}}(\varepsilon+i0^+)=H_{\mathrm{A}}^*(\varepsilon+i0^-)$ for $|\varepsilon|>|\Delta_L|$ stemming from Eqs. (5) and (6) leads to cast Eq. (2) in the same form as Eq. (7), where the sum over Γ_R^p (Γ_A^p) is replaced by a contour along the upper (lower) real axis range $\varepsilon\in[|\Delta_L|;\infty]$. Finally, the analyticity of $H_{\mathrm{R}}(z;\chi)$ and $H_{\mathrm{A}}(z;\chi)$ allows one to merge the above two contributions into

$$J(\chi)=-\frac{4ek_BT}{\hbar}\partial_\chi\sum_{m=0}^{\infty}\mathrm{Re}\ln(D_{\mathrm{R}}(iw_m;\chi)), \tag{8}$$

where $w_m=(2m+1)\pi/\beta_L$ are the Matsubara frequencies in units of $E_L/\hbar$. The relation $H_{\mathrm{A}}(-iw_n;\chi)=H_{\mathrm{R}}^*(iw_n;\chi)$ has been used.

Equation (8), combined with Eq. (5), gives the Josephson current in terms of the N-region scattering matrix S. Although equivalent to the original equations (1) and (2), Eq. (8) does not require determining the Andreev levels, yielding a major simplification in computing $J(\chi)$ for nonshort junctions.[13] We shall now show the rich physical scenario arising from a nonsymmetric S matrix. In order to illustrate this, we focus here on the case of a single conduction channel, where the S matrix is a 2×2 unitary matrix. Any $\mathsf{U}(2)$ matrix can be univocally written as

$$\mathsf{S}(\varepsilon)=e^{i\alpha(\varepsilon)}\begin{pmatrix}\rho(\varepsilon) & -i\tau(\varepsilon)\\ -i\tau^*(\varepsilon) & \rho^*(\varepsilon)\end{pmatrix}, \tag{9}$$

where $|\rho(\varepsilon)|^2+|\tau(\varepsilon)|^2=1$. Inserting Eq. (9) into Eq. (3), one obtains

$$D(\varepsilon;\chi)=1+A^2(\varepsilon)e^{2i\Psi(\varepsilon)}-2A(\varepsilon)e^{i\Psi(\varepsilon)}\{\mathrm{Re}(\rho(\varepsilon)\rho^*(-\varepsilon))+|\tau(\varepsilon)\tau(-\varepsilon)|\cos[\chi-\chi_0(\varepsilon)]. \tag{10}$$

where $\Psi(\varepsilon)=\alpha(\varepsilon)-\alpha(-\varepsilon)$. Notably, Eq. (10) shows that the phase difference χ is renormalized by a shift χ_0, related to the phase of the amplitude $\tau(\varepsilon)=|\tau(\varepsilon)|\exp(i\phi_\tau(\varepsilon))$ through the relation

$$\chi_0(\varepsilon)=\phi_\tau(\varepsilon)+\phi_\tau(-\varepsilon). \tag{11}$$

From Eqs. (11) it follows that χ_0 is nonvanishing only if τ is a complex number. At first sight, this property might seem a quite general feature of any quantum interferometer. This is, however, not the case, for the entries S_{ij} of the scattering matrix obey the microreversibility relation[12] $\mathsf{S}_{ij}|_B=\mathsf{S}_{ji}|_{-B}$, where B is the magnetic field. Thus, for any interferometer operating in the absence of magnetic field, the S matrix is symmetric, i.e., $\tau(\varepsilon)$ is real [see Eq. (9)]. One thus has $\chi_0=0$ and the system always behaves as a 0 junction. By contrast, if $B\neq 0$, the time-reversal symmetry (TRS) is broken, opening the possibility to the asymmetry of the S matrix, and hence to a $\chi_0\neq 0$. Importantly, $B\neq 0$ is a necessary, but not sufficient condition to have a π state: in a symmetric ring threaded by a uniform B, for instance, S is still symmetric and one has a 0 junction. If, however, the interferometer is suitably designed, an appropriate tuning of its parameters can lead to $\chi_0=\pi$, inducing a switching to a π state.

The electromagnetostatic AB interferometer (see Fig. 1) is an illuminating example to describe this effect. The explicit expression for the AB ring S matrix can be obtained with standard techniques[14] by combining the scattering matrices describing the Y junctions with the propagation matrix along the ballistic arms. For simplicity we neglect here band curvature, fringe field effects, and spin-orbit interaction. Each contact is described by the 3×3 Y-junction matrix S^Y,[15]

with entries $S^Y_{11}=-\cos\gamma$, $S^Y_{12}=S^Y_{13}=S^Y_{21}=S^Y_{31}=\sin\gamma/\sqrt{2}$, $S^Y_{22}=S^Y_{33}=(\cos\gamma-1)/2$, and $S^Y_{23}=S^Y_{32}=(\cos\gamma+1)/2$, where the parameter $\gamma\in[0;\pi/2]$ accounts for the contact transmission, with $\gamma=\pi/2$ describing a fully transmitting contact and $\gamma\to 0$ the tunnel limit.[16] The transmission of the two contacts will be assumed equal. The propagation along the two arms leads to the *AB* interferometry effect; right movers, for instance, acquire a phase $\exp(i(kL-\phi/2))$ along arm 1, and $\exp(i(kL+u+\phi/2))$ along arm 2, where $\phi=2\pi e\Phi_B/h$ and $u=eV_G/E_L$ (see Fig. 1), similarly for left movers. After lengthy but standard algebra, one can compute the S matrix (9) and the phase shift χ_0, which turns out to fulfill

$$\cos\chi_0(\varepsilon)=\frac{\mathrm{Re}\,\tau_P(\varepsilon)\mathrm{Re}\,\tau_P(-\varepsilon)-\mathrm{Im}\,\tau_P(\varepsilon)\mathrm{Im}\,\tau_P(-\varepsilon)}{|\tau_P(\varepsilon)\tau_P(-\varepsilon)|},\tag{12}$$

where $i\tau_P(\varepsilon)=\Sigma_{s=\pm}sC_s\exp[is(\varepsilon+\kappa'_F)]$, $C_\pm=\cos[(u\pm\phi)/2]$, and $\kappa'_F=k_FL+u/2$, with k_F the Fermi wave vector. Notice that χ_0 is independent of the contact transmission. For the purely electrostatic *AB* effect ($\phi=0$ and $u\neq 0$), we obtain $\chi_0=0$, as expected from the preservation of TRS. Moreover, Eq. (12) yields $\chi_0=0$, also for the purely magnetic *AB* effect ($u=0$ and $\phi\neq 0$): this is due to the additional relation $S_{12}|_B=S_{12}|_{-B}$, which holds in a symmetric ring if $u=0$. Although this relation breaks down if the ring is realized asymmetrically, the armlength is not a tunable quantity. However, Eq. (12) indicates that a much simpler way to achieve a controllable π state is to combine the magnetic flux and the gate voltage: when both $\phi\neq 0$ and $u\neq 0$, a phase $\chi_0\neq 0$ arises. Notice that, in this case, a Josephson current can flow even if $\chi=0$: if TRS is broken, the amplitude of processes bringing Cooper pairs from right to left lead are not necessarily compensated by those related to the opposite direction.

By substituting the S matrix into Eq. (10), and by performing the analytic continuation D_R as discussed above, the Josephson current is determined by Eq. (8). We shall now discuss the results. Figure 2 displays the switching of $J(\chi)$ from 0 to π-junction behavior, for a setup with $|\Delta|=2E_L$ and contact transmission 1/2 ($\gamma=\pi/3$) which corresponds, e.g., to a InGaAs ring with $L\sim 600$ nm[7] contacted to Nb leads, at zero temperature.[17] In particular, Fig. 2(a) shows J as a function of the phase difference χ: when $\phi=0$ and $u=0$, the junction is in a 0 state; by applying a gate voltage $u=0.8\pi$ the current is strongly suppressed (dotted curve), although its sign is always positive; however, when a magnetic flux $\phi=0.8\pi$ is also introduced, the current sign is reversed (dashed curve). Figure 2(b) and Fig. 2(c) refer to the Josephson current for $\chi=0$, and show that its sign can be reversed by tuning either the magnetic flux [Fig. 2(b)] or the gate voltage [Fig. 2(c)]. Notably, the curves of Fig. 2(b) demonstrate the crucial role of the gate voltage: for $u=0$, although J switches its sign upon varying the flux, the amplitude of the current is very small (solid curve); the latter is enhanced by increasing u (dotted and dashed curves).[18] The curves of Fig. 2(c) refer to different values of magnetic flux; in particular, when no magnetic flux is present (solid curve) the TRS yields $J(\chi=0)\equiv 0$ independent of the gate voltage u, whereas when $\phi\neq 0$ a supercurrent can flow and its sign varies with u

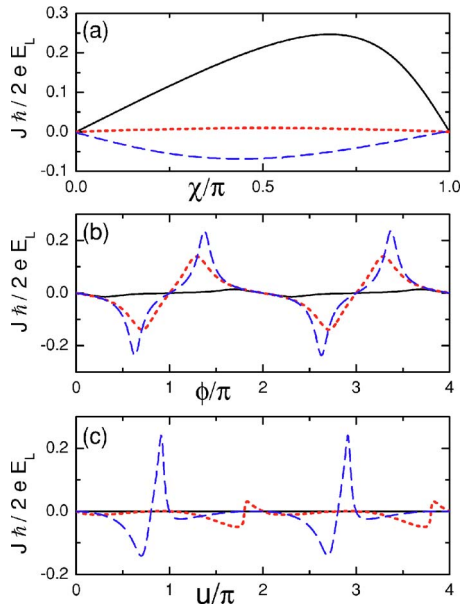

FIG. 2. (Color online) Sign switching of the Josephson current J for the setup of Fig. 1 with $|\Delta|=2E_L$, $k_FL=60$, and contact transmission 1/2 ($\gamma=\pi/3$). (a) $j(\chi)$ for $\phi=0$ and $u=0$ (solid), for $\phi=0$ and $u=0.8\pi$ (dotted), and for $\phi=0.8\pi$ and $u=0.8\pi$ (dashed); (b) $j(\chi=0)$ vs ϕ for different values of the gate voltage: $u=\pi/20$ (dotted), $u=\pi/2$ (dashed), and $u=1.2\pi$ (solid); (c) $j(\chi=0)$ vs u for different values of magnetic flux: $\phi=0$ (solid), $\phi=0.1\pi$ (dotted), and $\phi=0.9\pi$ (dashed).

(dotted curve), with a strong enhancement when the flux approaches $\phi=\pi$. The whole behavior of the Josephson current $J(\chi=0)$ as a function of u and ϕ is displayed in Fig. 3. The supercurrent exhibits lobes of alternate signs whose nodes are located around some special values of ϕ and u. The latter can be roughly estimated through the condition $\cos\chi_0\simeq -1$ [see Eq. (12)], yielding $\phi\simeq(2m_1+1)\pi$, $u\simeq(2m_2+1)\pi$, and $u\simeq 2(\pi m_3-k_FL)$, with integer m_j's.[19] The sign reversal is thus easily controlled around these values. This proves the full tunability of the supercurrent through electromagnetostatic *AB* effect.

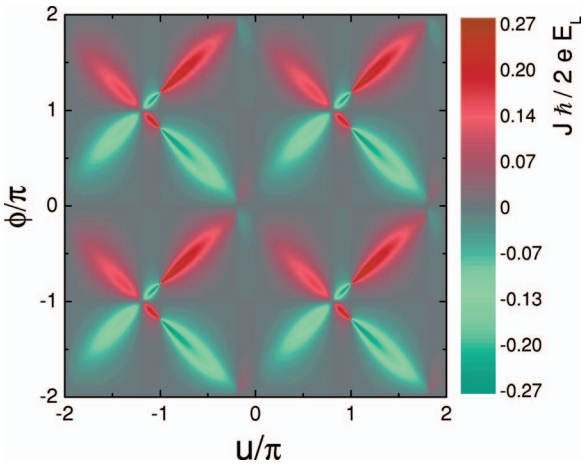

FIG. 3. (Color) Dimensionless Josephson current vs u and ϕ for an *AB* ring with $|\Delta|=2E_L$, $k_FL=60$, $\gamma=\pi/3$, and $\chi=0$.

In conclusion, we have proposed Aharonov-Bohm interferometry as a tool to realize a controllable Josephson π junction. While the magnitude of the supercurrent can be tuned by either the electrostatic or the magnetic *AB* effect, its sign can be controlled only if time-reversal symmetry is broken. We have also shown that a magnetic field alone does not provide an efficient tuning of the supercurrent [see Fig. 2(b)]. By contrast, the combined use of magnetic and electric field enhances the supercurrent amplitude, allowing a full control of the junction. In addition, our results also imply that *supercurrent* measurements can be used to determine the asymmetry of the S matrix; indeed the ordinary dc current in a ring contacted to normal leads only depends on the transmission coefficient $\mathcal{T}=|\tau|^2=|\tau^*|^2$, and the asymmetry cannot be probed.

We acknowledge stimulating discussions with R. Fazio, F. Carillo, A. Khaetskii, M. Governale, H. Grabert, and A. Saracco, and partial financial support by HYSWITCH EU Project and MIUR FIRB Project No. RBNE01FSWY.

[1] T. D. Clark, R. J. Prance, and A. D. C. Grassie, J. Appl. Phys. **51**, 2736 (1980).

[2] Y.-J. Doh *et al.*, Science **309**, 272 (2005); P. Jarillo-Herrero, J. van Dam, and L. P. Kouwenhoven, Nature (London) **439**, 953 (2006); T. Akazaki *et al.*, Appl. Phys. Lett. **68**, 418 (1996).

[3] V. V. Ryazanov, V. A. Oboznov, A. Y. Rusanov, A. V. Veretennikov, A. A. Golubov, and J. Aarts, Phys. Rev. Lett. **86**, 2427 (2001); T. Kontos, M. Aprili, J. Lesueur, F. Genet, B. Stephanidis, and R. Boursier, *ibid.* **89**, 137007 (2002).

[4] B. J. van Wees, K.-M. H. Lenssen, and C. J. P. M. Harmans, Phys. Rev. B **44**, 470 (1991); F. K. Wilhelm, G. Schön, and A. D. Zaikin, Phys. Rev. Lett. **81**, 1682 (1998); A. F. Volkov, *ibid.* **74**, 4730 (1995); J. J. A. Baselmans *et al.*, Nature (London) **397**, 43 (1999); F. Giazotto *et al.*, Rev. Mod. Phys. **78**, 217 (2006); P. Samuelsson, J. Lantz, V. S. Shumeiko, and G. Wendin, Phys. Rev. B **62**, 1319 (2000).

[5] L. I. Glazman, and K. A. Matveev, JETP Lett. **49**, 659 (1989); J. A. van Dam *et al.*, Nature (London) **442**, 667 (2006); F. Siano and R. Egger, Phys. Rev. Lett. **93**, 047002 (2004); A. V. Rozhkov, D. P. Arovas, and F. Guinea, Phys. Rev. B **64**, 233301 (2001).

[6] Y. Makhlin, G. Schön, and A. Shnirman, Rev. Mod. Phys. **73**, 357 (2001).

[7] F. Carillo *et al.*, Physica E (Amsterdam) **32**, 53 (2006).

[8] H. Takayanagi, T. Akazaki, and J. Nitta, Phys. Rev. Lett. **75**, 3533 (1995).

[9] C. W. J. Beenakker, Phys. Rev. Lett. **67**, 3836 (1991).

[10] G. Wendin and V. S. Shumeiko, Superlattices Microstruct. **20**, 569 (1996).

[11] C. Ishii, Prog. Theor. Phys. **44**, 1525 (1970); A. V. Svidzinskii, T. N. Antsygina, and E. N. Bratus, Sov. Phys. JETP **34**, 860 (1972).

[12] P. Roman, *Advanced Quantum Theory* (Addison-Wesley, Reading, 1965).

[13] For $|\Delta_L| \ll 1$ and a symmetric S, the result of Ref. 9 is recovered. In the case of a quantum point contact, Eq. (8) reduces to the result of A. Furusaki, H. Takayanagi, and M. Tsukada, Phys. Rev. Lett. **67**, 132 (1991).

[14] M. Cahay, S. Bandyopadhyay, and H. L. Grubin, Phys. Rev. B **39**, 12989 (1989); D. Takai and K. Ohta, *ibid.* **48**, 1537 (1993).

[15] M. Büttiker, Y. Imry, and M. Ya. Azbel, Phys. Rev. A **30**, 1982 (1984); Y. Gefen, Y. Imry, and M. Ya. Azbel, Phys. Rev. Lett. **52**, 129 (1984).

[16] R. Fazio, F. W. J. Hekking, and A. A. Odintsov, Phys. Rev. Lett. **74**, 1843 (1995); Phys. Rev. B **53**, 6653 (1996).

[17] We expect our results to be robust to thermal fluctuations for $T < T_0 = E_L/k_B \sim 10$ K.

[18] In the present setup, the channel current unit $2eE_L/\hbar$ corresponds to about 300 nA.

[19] For a ring of $L \simeq 600$ nm, an elementary magnetic flux corresponds to $B \sim 10^{-2}$ T, i.e., much lower than the critical field B_{c2} of (Nb) leads.